Journal of Visualized Experiments

Native cell membrane nanoparticles system for membrane protein-protein interaction analysis

--Manuscript Draft--

Article Type:	Invited Methods Collection - JoVE Produced Video
Manuscript Number:	JoVE61298R3
Full Title:	Native cell membrane nanoparticles system for membrane protein-protein interaction analysis
Keywords:	SMALP, Native Cell Membrane Nanoparticles system, Membrane protein, Memtein, Electron microscopy, Protein-protein interaction
Corresponding Author:	Youzhong Guo Virginia Commonwealth University Richmond, Virginia UNITED STATES
Corresponding Author's Institution:	Virginia Commonwealth University
Corresponding Author E-Mail:	yguo4@vcu.edu
Order of Authors:	Kyle Kroeck
	Weihua Qiu
	Claudio Catalano
	Thi Kim Hoang Trinh
	Youzhong Guo
Additional Information:	
Question	**Response**
Please indicate whether this article will be Standard Access or Open Access.	Standard Access (US$2,400)
Please indicate the **city, state/province, and country** where this article will be **filmed**. Please do not use abbreviations.	Richmond, Virginia, USA

TITLE:

Native Cell Membrane Nanoparticles System for Membrane Protein-Protein Interaction Analysis

AUTHORS & AFFILIATIONS:

Kyle G. Kroeck[1,2], Weihua Qiu[1,2], Claudio Catalano[1,2], Thi Kim Hoang Trinh[1,2], Youzhong Guo[1,2]

[1]Department of Medicinal Chemistry, School of Pharmacy, Virginia Commonwealth University, Richmond, VA, USA

[2]Institute for Structural Biology, Drug Discovery and Development, School of Pharmacy, Virginia Commonwealth University, Richmond, VA, USA

Email addresses of authors:

Kyle G. Kroeck (kroeckkg@vcu.edu)
Weihua Qiu (wqiu@vcu.edu)
Claudio Catalano (ccatalano@vcu.edu)
Thi Kim Hoang Trinh (trinhtk2@vcu.edu)

Corresponding author:

Youzhong Guo (yguo4@vcu.edu)

KEYWORDS:

SMALP, native cell membrane nanoparticles system, membrane protein, memtein, nanoparticles, oligomeric state determination

SUMMARY:

Presented here is a protocol for the determination of oligomeric state of membrane proteins that utilizes a native cell membrane nanoparticle system in conjunction with electron microscopy.

ABSTRACT:

Protein-protein interactions in cell membrane systems play crucial roles in a wide range of biological processes- from cell-to-cell interactions to signal transduction; from sensing environmental signals to biological response; from metabolic regulation to developmental control. Accurate structural information of protein-protein interactions is crucial for understanding the molecular mechanisms of membrane protein complexes and for the design of highly specific molecules to modulate these proteins. Many in vivo and in vitro approaches have been developed for the detection and analysis of protein-protein interactions. Among them the structural biology approach is unique in that it can provide direct structural information of protein-protein interactions at the atomic level. However, current membrane protein structural biology is still largely limited to detergent-based methods. The major drawback of detergent-based methods is that they often dissociate or denature membrane protein complexes once their native lipid bilayer environment is removed by detergent molecules. We have been developing a detergent free native cell membrane nanoparticle system for membrane protein structural biology. Here, we demonstrate the use of this system in the analysis of protein-protein interactions on the cell membrane with a case study of the oligomeric state of AcrB.

INTRODUCTION:

Protein-protein interactions (PPI) play pivotal roles throughout biology, from the maintenance of the structure and function of proteins to the regulation of entire systems. PPIs come in many different forms and can be categorized based on what types of interactions they form. One such categorization is homooligomeric or heterooligomeric, based on whether the interactions are between identical subunits or different proteins acting as subunits. Another categorization is based on the strength of the interaction if the interactions leads to the formation of stable complexes or transient complex states. Structural information about the PPIs between proteins is crucial in understanding the mechanism by which proteins carry out their function. It has been estimated that over 80% of proteins rely on complex formation in order to carry out their functional roles[1]. Given the percentage of proteins observed to be reliant on PPIs for proper innate functioning their significance in biology is readily apparent, yet being able to properly investigate the proteins that engage in these interactions has remained challenging due to limitations in the techniques available to experimentally observe when proteins are forming PPIs.

There is a high degree of disagreement between the results for many experimentally determined PPIs due to the high amount of noise, false positives, and false negatives that are derived from many of the currently available PPI determining techniques. This is particularly so for the yeast two-hybrid (Y2H) system, tandem affinity purification-mass spectrometry (TAP-MS), and fluorescence resonance energy transfer (FRET), which represent three of the most commonly used methods for PPI determination[2-7]. In comparison, protein structural biology techniques, such as nuclear magnetic resonance (NMR), X-ray crystallography and electron microscopy (EM), can be used to gain high-resolution structural information about protein-protein interactions down to the atomic level and allow for the direct visual confirmation of the interactions occurring for a target protein of interest. All of the currently available non-structure based PPI determining research techniques (e.g., Y2H, TAP-MS, and FRET) lack this ability and additionally suffer from having difficulty in identifying weak and transient interactions between proteins[5]. These shortcomings are further enhanced when studying membrane proteins due to the added complexity brought on by the additional variable of the lipid environment that influences the formation of proper quaternary structure and heteromeric complex assembly.

Membrane proteins make up a large portion of the proteome and are known to play many crucial roles in proper cell functioning within all living organisms. Despite the fact that membrane proteins are estimated to make up 27% of the human genome and constitute ~60% of all current drug targets there is a major anomaly in the number of solved models for membrane proteins which make up only ~2.2% of all published protein structures[8-10]. The primary cause of the discrepancy in the availability of structural information lies in the intrinsic properties of membrane proteins themselves. Due to their poor solubility, reliance on interactions with a lipid environment for maintaining native structure and function, and various physicochemical properties of the lipid membrane itself, membrane proteins continue to represent a substantial problem when implementing structural biology techniques to study them. Of these intrinsic properties, the most important for obtaining accurate structural information is the requirement of having interactions with their natural lipid environment for them to maintain their native

structure and function. The lipid environment is such an integral part of the structure and function of membrane proteins that the concept of memtein (a combination of the words membrane and protein) has been proposed as the fundamental unit of membrane-protein structure and function[11]. Despite the importance of lipid-protein interactions the currently available structure-based PPI determination techniques often require that the proteins being studied be soluble or be solubilized with detergents. Exposure to harsh detergents can denature the proteins or cause false positives and negatives due to delipidation, which can induce aggregation, denaturation of protein, dissociation of non-covalent interactions, and formation of artificial oligomeric states. Due to the necessity of maintaining a natural lipid environment for accurate determination of the native oligomeric state of membrane proteins we have developed a Native Cell Membrane Nanoparticles system (NCMNs)[12] based on the previously reported Styrene Maleic Acid Lipid Particles (SMALP)[13] method.

SMALP uses styrene maleic acid copolymer as a membrane active polymer to extract and solubilize membrane proteins. Poly(Styrene-co-Maleic Acid) (SMA) is a unique amphiphilic polymer due to its hydrophobic styrene moiety and diametrically opposing hydrophilic maleic acid moiety. It forms nanoparticles by adsorbing to, destabilizing, and disrupting the cell membrane in a pH-dependent mechanism[14]. This functional activity of SMA is what allows it to be utilized as a detergent-free system for membrane protein extraction and solubilization. The NCMN system is distinct from the SMALP system in several aspects. The most unique feature of the NCMN system is that it has a membrane active polymer library with a multitude of polymers that have unique properties that make them suitable for the isolation of many different membrane proteins that require different conditions for stability and native functioning. The NCMN system also has different protocols compared to the SMALP method when it comes to preparing the nanoparticles. One such example is that NCMNs use a single-step nickel affinity column purification for high-resolution structure determination; the effect of these different protocols can be observed when comparing the NCMNs protocol, which generated 3.2 and 3.0 Å cryo-EM AcrB structures, with a similar study using the SMALP method, which resulted in a cryo-EM AcrB structure at an 8.8 Å resolution[12,15]. These unique features of the NCMN system are the improvements made on the previously established SMALP method and make it an ideal candidate for the study of PPIs.

The multidrug efflux transporter AcrB exists as functional homotrimer in *E. coli*.[12] A mutagenic analysis suggested that a single P223G point mutation, located on a loop that is responsible for the stability of the AcrB trimer, destabilizes the trimer state and yields an AcrB monomer when prepared with the detergent DDM, which could be detected with native blue gel electrophoresis[16]. However, the FRET analysis of the AcrB-P223G mutant suggested that when in the native cell membrane lipid bilayer environment, the majority of mutant AcrB-P223G still existed as a trimer and that the expression levels for both wild type AcrB and AcrB-P223G are similar. Yet despite the FRET analysis results, an activity assay for the mutant transporter showed that activity dramatically decreased when compared to the wild type[16]. Although FRET technology has been popularly used for the analysis of protein-protein interactions, research has shown that it can frequently give false positives[17-20].

Recently high-resolution cryo-EM structures of the AcrB trimer were determined which showed the interaction of AcrB with its associated native cell membrane lipid bilayer through the use of the NCMNs[12]. In principle, the NCMNs can readily be utilized for the analysis of protein-protein interactions found on the native cell membrane. In a test of this system, experiments were carried out to directly observe the oligomeric state of AcrB-P223G with the use of native cell membrane nanoparticles and negative staining electron microscopy. In order to compare with the wild type AcrB nanoparticles, we used the same membrane active polymer (SMA2000 made in our laboratory, which is indexed as NCMNP1-1 in the NCMN library) used for high-resolution cryo-EM structure determination of AcrB and alternative polymers found in the NCMNs library[12]. Based on the previously reported results, it was expected that the majority of the AcrB-P223G mutant would exist in the form of trimeric native cell membrane nanoparticles[21]. However, no AcrB trimers were found present in the sample, such as the ones that were observed with the wild type AcrB. This suggests the majority of AcrB-P223G does not form trimers on the native cell membrane as previously suggested.

Here we report a detailed analysis of the mutant *E. coli* AcrB-P223G in a comparison with the wild type *E. coli* AcrB using the NCMNs. This case study of AcrB suggests NCMNs is a good system for protein-protein interaction analysis.

PROTOCOL:

1. Protein expression

1.1. Inoculate 15 mL of Terrific Broth (TB) media with antibiotics specific to plasmids with BL21(DE3) pLysS cells containing the AcrB expressing plasmids in 50 mL tubes overnight at 37 °C with shaking at 250 rpm.

1.2. Check the optical density of the overnight culture at 600 nm (OD_{600}) and ensure that it is over 2.0.

1.3. Dilute 5 mL of cell culture into 1 L of TB media containing antibiotics specific to plasmids and incubate at 37 °C with shaking until OD_{600}=0.8 and then induce with IPTG that has a final concentration of 1 mM.

1.4. Carry out induction at 20 °C with shaking for 20 h.

1.5. Pellet down the cells using centrifugation for 15 min at 4 °C and 4,000 *x g*.

2. Cell lysis and membrane isolation

2.1. Resuspend the cell pellet in Buffer A (**Table 1,** use DDM Buffer A or NCMNs Buffer A depending on purification scheme that is to follow) using 80 mL for every 20 g of the cell pellet.

2.2. Homogenize the resuspended cell pellets by using a glass Dounce homogenizer at 4 °C or if

at room temperature be sure to put on ice immediately after.

2.3. Transfer the sample into a metal beaker on ice and lyse the cells by loading them into a high-pressure homogenizer at 4 °C and 1,500 bar.

2.3.1. Repeat the process of loading the cells into the homogenizer and allowing them to pass through the homogenizer for 3-4 cycles or until the lysate begins to clarify.

2.4. Centrifuge the lysate at 15,000 *x g* for 30 min at 4 °C.

2.5. Collect the supernatant and load into ultracentrifuge tubes and centrifuge at 215,000 *x g* for 1 h at 4 °C.

2.6. Discard the supernatant and collect the membrane pellets from the ultracentrifuge tubes. Store any excess membrane pellet at -80 °C.

3. Preparation of native cell membrane nanoparticles

3.1. Resuspend 1 g of membrane pellet in 10 mL NCMNs Buffer A (**Table 1**).

3.2. Homogenize the resuspended cell membrane sample with a glass Dounce homogenizer at 20 °C.

3.3. Transfer the suspended membrane sample to a 50 mL polypropylene tube and add membrane active polymers stock solution and additional NCMNs Buffer A to bring the sample to a final concentration of 2.5% (w/v) membrane active polymer (NCMNP1-1 or NCMNP5-2).

NOTE: Stock solutions of membrane active polymers should be made in double distilled water and can be kept at varying concentrations, but typically 10% (w/v).

3.4. Shake the sample for 2 h at 20 °C.

3.5. Load the sample into an ultracentrifuge and spin at 150,000 *x g* for 1 h at 20 °C.

3.6. While the sample is being ultra-centrifuged begin to equilibrate a 5 mL Ni-NTA column with 25 mL of NCMNs Buffer A.

3.7. Collect the supernatant after ultracentrifugation is complete and load it onto 5 mL of Ni-NTA column at room temperature with a flow rate of 0.5 mL/min using a syringe pump.

3.8. Wash fast protein liquid chromatography (FPLC) lines with enough NCMNs Buffer B (**Table 1**) to completely flush the system and then connect the column to the FPLC machine.

3.9. Wash the column with 30 mL of NCMNs Buffer B with a flow rate of 1 mL/min and collect the

flow through.

3.10. Wash the column with 30 mL of NCMNs Buffer C (**Table 1**) with a flow rate of 1 mL/min and collect the flow through.

3.11. Elute the protein with 20 mL of NCMNs Buffer D (**Table 1**) at a flow rate of 0.5 mL/min and collect the sample using a fraction collector and the fractions each being set to 1.0 mL.

3.12. Store the protein samples at 4 °C.

3.13. Run an SDS-PAGE gel electrophoresis assay in order to check the samples that correspond to peaks observed on the FPLC elution graph.

4. SDS-PAGE gel electrophoresis

4.1. Prepare the casting chamber by clamping the glass to the casting apparatus.

4.2. Prepare the 12% separation gel according to the recipe listed in **Table 1**.

NOTE: Once TEMED is added the gel will polymerize quickly so only add this once ready to pour the gel.

4.3. Pour the gel, leaving 2 cm below the bottom of the comb for the stacking gel.

4.4. Remove any bubbles by layering the top of the gel with 100% isopropanol and wait for the separation gel to polymerize.

4.5. Remove the isopropanol and wash out any traces of the isopropanol with distilled water.

4.6. Prepare the stacking gel according to the recipe listed in **Table 1**.

NOTE: Once TEMED is added the gel will polymerize quickly so only add this once ready to pour the gel.

4.7. Pour the stacking gel on top of the separation gel.

4.8. Add a comb to the chamber to form the wells and wait for the stacking gel to completely polymerize.

4.9. Place 1 µL of 1 M DTT into a microcentrifuge tube for each fraction sample that needs to be run on the gel.

4.10. Add 7 µL of 4x loading buffer to each tube as well.

4.11. Add 20 µL of sample from the fractions that need to be run on the gel to each microcentrifuge tube.

4.12. Vortex the tubes containing the samples.

4.13. Spin down the sample tubes using a tabletop microcentrifuge for 3 s and make sure all the sample has returned to bottom of the tubes.

4.14. Prepare the gel electrophoresis cell by securing a 12% polyacrylamide gel cassette into place and filling the inner and outer chambers of the cell with Tris-acetate-EDTA (TAE) Buffer (**Table 1**).

4.15. Load the molecular weight marker into the first lane of the gel with the appropriate volume required by its instructions.

4.16. Load 28 µL of the sample from each tube mixed with DTT and loading buffer.

4.17. Place the lid of the electrophoresis cell on top of the box and plug the lid into the power supply.

4.18. Turn on the power supply and set it to 100 V and allow it to run for 20 min.

4.19. After 20 min, increase the power supply current to 140 V and continue to run it for another 30-40 min or until the band of loading buffer dye reaches the bottom of the gel cassette.

4.20. After completing electrophoresis stain and de-stain the gel to visualize the protein bands contained within the gel.

5. Protein purification using DDM

NOTE: The purpose of carrying out this purification process is to serve as a control for the experiments utilizing the membrane active polymers.

5.1. Resuspend 6-10 g of membrane pellet, from step 2.6, in DDM Buffer A (**Table 1**) using 5 mL/g of membrane pellet.

5.2. Homogenize the resuspended sample with a glass Dounce homogenizer at 4 °C or if at room temperature be sure to put on ice immediately after.

5.3. Transfer sample to a 50 mL of polypropylene tube and add DDM and additional DDM Buffer A to bring the sample to a final concentration of 2% DDM.

5.4. Shake the sample for 2 h at 4 °C.

5.5. Load the sample into ultracentrifuge tubes and centrifuge for 1 h at 4 °C and 150,000 *x g*.

5.6. While sample is being ultra-centrifuged begin to prepare the 5 mL of Ni-NTA column by washing with 25 mL of DDM Buffer A (**Table 1**).

5.7. After ultracentrifugation is complete, collect the supernatant and load it onto the 5 mL Ni-NTA column at 4 °C with a flow rate of 0.5 mL/min using a syringe pump.

5.8. Wash FPLC lines with enough DDM Buffer B + 0.05% DDM (**Table 1**) to completely flush the system and then attach the column to the FPLC machine.

5.9. Wash the column with 30 mL of DDM Buffer B + 0.05% DDM with a flow rate of 1 mL/min and collect the flow through.

5.10. Wash the column with 30 mL of DDM Buffer C + 0.05% DDM (**Table 1**) with a flow rate of 1 mL/min and collect the flow through.

5.11. Elute the protein with 20 mL of DDM Buffer D + 0.05% DDM (**Table 1**) at a flow rate of 0.5 mL/min and collect the flow through using a fraction collector and the fractions each being set to 1.0 mL.

5.12. Select the fractions containing the elution peak for pooling and concentrating by using a centrifugal concentrator and centrifuging at 4,000 *x g* and 4 °C until reaching 500 µL.

5.13. Using a 500 µL loop load the sample into the FPLC machine and then onto the 25 mL size exclusion column at 4 °C. Elute using 30 mL of DDM Buffer E + 0.05% DDM (**Table 1**) at a flow rate of 0.5 mL/min and collect as fractions with the fraction sizes set to being 0.5 mL per a fraction.

5.14. Take the fractions and measure the protein concentration using 280 nm absorbance to confirm UV-Vis curve from the FPLC elution graph.

5.15. Collect 20 µL from each sample fraction that correspond to peaks observed on the FPLC elution graph and were confirmed to be accurate with the absorbance test.

5.16. Freeze the remainder of those sample fractions using liquid nitrogen or dry ice in desired aliquots and store protein samples at -80 °C.

5.17. Run an SDS-PAGE gel electrophoresis assay as previously described to check the samples that correspond to peaks observed on the FPLC elution graph.

6. Negative stain grid preparation

6.1. Place the grids that are going to be used for the sample preparation on a glass slide wrapped in filter paper with the carbon side facing up.

6.2. Place the glass slide with the electron microscope grids into the chamber of a glow discharger between the two electrodes and replace the glass lid making sure it is centered and well-sealed.

6.3. Run the glow discharging machine and make sure that the purple light generated by the plasma is visible.

6.4. When the machine is done running, wait until the chamber has reached atmospheric pressure to remove the glass lid and then return the slide with the grids to the bench where samples will be loaded onto them.

6.5. Adjust the concentration of the purified protein samples to about 0.1 mg/mL by either diluting the sample with the appropriate buffer or concentrating using a centrifugal concentrator.

6.6. Load 3.5 µL of protein sample onto the 10 nm thick carbon grid and wait for 1 min.

6.7. Remove the liquid from the surface of the EM grid with a filter paper.

6.8. Wash the grid surface 3x by picking up 3 µL droplets of water with the grid and removing the water from the grid with filter paper in between picking up each droplet.

6.9. Wash the grid surface 2x by picking up 3 µL droplets of fresh, filtered 2% uranium acetate and remove the wash solutions on the grid with filter paper in between picking up each droplet.

6.10. Stain the grid with a 3 µL droplet of fresh, filtered 2% uranium acetate for 1 min.

6.11. Remove the uranium acetate solution on the surface of the EM grid with filter paper and air dry the grid for at least 1 min.

6.12. Store the grid in a grid box for the later use.

7. EM imaging

7.1. Load the prepared grid into the grid holder at a safe workbench.

7.2. Prepare the microscope by placing the microscopes dewar into a polystyrene box and fill the dewar 3/4th full of liquid nitrogen.

7.3. Confirm that the rubber cover of the microscope window is covering it and then load the dewar onto the microscope by placing the copper wires into the dewar until it fits on the platform.

7.4. Fill the remainder of the dewar with liquid nitrogen and place a cap on top of the dewar to cover it.

7.5. Turn on the high tension, condition the microscope, and wait for the microscope to warm up and establish a safe vacuum level for use.

7.6. Once the microscope is ready open the column valve and confirm the beam is present by removing the rubber cover on the microscope window.

7.7. Check the beam stigmation by spreading in and out by adjusting the intensity of the beam. If astigmatism is present the beam will have an elliptical shape as one rotate away from cross-over and the beam should be the same oval shape on both sides.

7.8. Adjust the microscope binoculars to be the right height and distance as per the eyes of the observer.

7.9. Check the beam positioning for **Search**, **Focus**, and **Exposure** modes by cycling through all three modes until the beam is center in each.

7.10. Close the column valve and proceed to load the grid holder into the electron microscope.

7.11. Adjust the microscope to eucentric height by using the microscopes wobbler feature and adjusting the movement of the stage using the Z-axis until there is no side-to-side motion of the sample in the center.

7.12. Using the low dose **Search** mode on the microscope search the grid for a desirable area of reasonable contrast with sample molecules present to focus on the sample.

7.13. Focus on the sample in **Focus** mode by using a high step size until the sample is seen and then decrease steps to find the correct focus level.

7.14. Zero and blank the beam and then be sure the rubber pad is covering the microscope window.

7.15. Using the **Exposure** mode take the image of the desired grid area for a 1 s exposure at 62,000x magnification and check the obtained image.

7.16. When done imaging a grid close the column valves and remove the grid holder from the column.

7.17. When finished imaging all grids of interest shutdown the microscope by turning off the filament power and removing the liquid nitrogen dewar from the microscope.

7.18. Place something to absorb moisture on the stand where the dewar sat to catch condensation from the copper coils of the microscope.

7.19. Activate the **Cryo Cycle** mode and make sure the turbo pump is turned off.

REPRESENTATIVE RESULTS:

Using the procedures presented here, samples of *E. coli* AcrB wild type and *E. coli* mutant AcrB-P223G were purified. The samples were then adsorbed to carbon negative stain electron microscopy grids and stained using uranyl acetate with the side blotting method[22]. Negative stain images were collected using transmission electron microscopy. The negative stain image for the AcrB wild type sample purified with DDM reveals a homogenous solution of monodispersed particles with the protein displaying a well-defined trimeric quartenary structure (**Figure 1A**). These trimeric structures correspond with the observed size exclusion chromatogram when purified (**Supplementary Figure 1**). In comparison, when looking at the negative stain image for the AcrB-P223G mutant, also purified with DDM, one can observe a heterogeneous solution of polydispersed nanoparticles with a propensity towards aggregation, but no observable native trimers (**Figure 1B**). These results are also supported by the observed elution profile when carrying out size exclusion chromatography (**Supplementary Figure 1**). To determine if the lack of trimeric state proteins for the mutant was due to treatment with detergent or solely caused by the destabilizing mutation of P223G the proteins were also purified using NCMNP1-1, one of the membrane active polymers within the NCMNs library. The negative stain image for the AcrB wild type sample purified with NCMNP1-1, again, reveals a homogenous solution of monodispersed particles with the protein displaying a well-defined trimeric quartenary structure (**Figure 1C**). And just like with the DDM purification, when the AcrB-P223G mutant is purified with NCMNP1-1 the negative stain image shows a heterogeneous solution of polydispersed nanoparticles with a propensity towards aggregation, but no observable native trimers (**Figure 1D**). To further confirm that the P223G mutation disrupts the AcrB trimer on the cell membrane a different polymer (NCMNP5-2) was selected from the proprietary NCMNs membrane active polymer library. NCMNP5-2 can form native cell membrane nanoparticles in much larger sizes, thus allowing multiple AcrB trimers to be imaged in a single native cell membrane particle. As a result, it was observed that multiple wild type AcrB trimers were contained in single particles (**Figure 1E**); however, no AcrB-P223G trimer particles like those formed by wild type AcrB were observed, even when looking at the large native cell membrane bilayer patches (**Figure 1F**). This suggests AcrB-P223G does not exist as a trimer on the cell membrane as previously suggested[21] and offers a logical explanation as to why AcrB-P223G shows a dramatic decline in activity when assayed[16]. To confirm the purity of the samples and presence of the correct protein, electrophoresis gels were run for all the purified protein samples. The resulting stains confirmed the presence of AcrB in all the samples with >95% purity and the location of the stain corresponded to the predicted molecular weight of AcrB (**Figure 1G**). The results from our study are inconsistent with the previously described FRET assay with regards to determining the oligomeric state of the membrane protein AcrB-P223G[16]. By utilizing membrane active polymers and electron microscopy as described in the protocol the native oligomeric state of the protein was directly observable. A more accurate determination of how the monomers of the protein interact with one another will require the determination of high-resolution cryo-EM structures.

FIGURE AND TABLE LEGENDS:

Figure 1: Negative stain and electrophoresis gel images of purified AcrB constructs. (**A**) Negative stain image taken for wild type AcrB purified with DDM. (**B**) Negative stain image taken for the AcrB-P223G protein construct purified with DDM. (**C**) Negative stain image taken for wild type AcrB purified with NCMNP1-1. (**D**) Negative stain image taken for AcrB-P223G construct purified with NCMNP1-1. (**E**) Negative stain image taken for wild type AcrB purified with NCMNP5-2 (the red box highlights some of the trimer nanoparticles observed in the image). (**F**) Negative stain image taken for AcrB-P223G purified with NCMNP5-2 (the green box highlights a portion of the lipid patches captured by NCMNP5-2 observed in the image). (**G**) SDS-PAGE gel run using the final products from the purifications of AcrB-P223G with DDM (Lane 1), NCMNP1-1 (lane2), (**H**) SDS-PAGE gel run using the final products from the purifications of AcrB-P223G with NCMNP5-2. (**I**) Zoom in of the highlighted features from Figure 1E. (**J**) Zoom in of the highlighted features from F. All the negative stain images in Figure 1 have the same scale bar of 50 nm.

Table 1: List of purification buffers used for column chromatography.

Supplementary Figure 1: Size exclusion chromatography elution profiles. (**A**) Overlay graph of the two elution profiles observed for the size exclusion chromatography experiments carried out when purifying with DDM and wild type AcrB (orange) and with DDM and the mutant AcrB-P223G (blue). (**B**) Column calibration profile for size exclusion column utilized for DDM experiments. 1: Thyroglobulin (Mr 669 000), 2: Ferritin (Mr 440 000), 3: Aldolase (Mr 158 000), 4: Conalbumin (Mr 75 000), 5: Ovalbumin (Mr 44 000), 6: Carbonic anhydrase (Mr 29 000), 7: Ribonuclease A (Mr 13 700).

DISCUSSION:

Protein-protein interactions are important for the integrity of the structure and function of membrane proteins. Many approaches have been developed to investigate protein-protein interactions. When compared with soluble proteins, membrane proteins and their PPIs are more difficult to study due to the unique intrinsic properties of membrane proteins. This difficulty mainly comes from the requirement of membrane proteins to be embedded in a native lipid bilayer environment for structural stability and functionality. This becomes problematic because in order to determine high resolution structures of the proteins they must be extracted from the cell membrane. FRET has been a popular technology to investigate protein-protein interactions on the cell membrane, however, the resolution is low and frequently produces false positives[17-20]. Here it is demonstrated, for the first time, that NCMNs can be used for studying membrane protein-protein interactions by structurally analyzing the wild type AcrB trimer and AcrB-P223G monomer on the native cell membrane and comparing results with the previous analysis using FRET. By comparing the electron microscopy single particle images of wild type AcrB and AcrB-P223G, it is suggested that the majority of AcrB-P223G does not form trimers on the *E.coli* cell membrane like the wild type AcrB protein when purified using membrane active polymers, like NCMNP1-1 and NCMNP5-2. We propose here that the results from the FRET analysis may be a false positive resulting from the resolution limitation of the FRET approach. The artificial disulfide bond that stabilized the AcrB-P223G trimer could also be an artifact that occurred in solution[21]. The negative stain images suggest that the P223G mutation prevented formation of the AcrB trimer and that the monomeric form of AcrB could not remain in the same conformation

observed when in its trimeric form. The loop that contains this mutation was previously shown to be absolutely critical for formation of the trimer through mutagenic and structural analysis, which showed its structural significance to be due to the interactions each loop forms by burying into the neighboring AcrB monomer[23].

By utilizing the native cell membrane nanoparticle system for protein-protein interaction detection and analysis one can directly detect the oligomeric state of a protein by keeping the membrane protein(s) in a truly native cell membrane environment, which can be used for gaining high resolution structural information at the atomic level through single particle cryo-EM analysis of the sample. The NCMN system helps avoid the frequent false positives and false negatives observed in PPI detection caused by treating samples with detergents[24]. These false results typically arise, because of the aggregation, denaturation of protein sample, dissociation of non-covalent interactions, and formation of artificial oligomeric states caused by the delipidation effects of detergents. Additionally, using structural analysis in conjunction with the NCMNs provides additional structural information and allows for the direct observation of molecular interactions, which are both critical to understanding PPIs and typically lost when utilizing previously established methods of PPI detection. This method has successfully been used for structural studies of wild type AcrB and could have wide applicability to other forms of structural analysis, such as X-ray crystallography and solid state NMR, and many different proteins being used in other research seeking to determine the interactions displayed by novel protein targets.

In order to obtain reproducible results with reasonable protein yields of high purity there are several critical steps in the purification process with membrane active polymers that must be followed. The first critical step is the process of membrane isolation, thus it is critical to centrifuge the cell lysate at 15,000 *x g* and follow this step with ultracentrifugation at 215,000 *x g* in order to truly isolate the cell membrane from the rest of the cell lysate. The next critical step is solubilizing the membrane fraction with membrane active polymers at a concentration of 2.5% at room temperature for two hours. Optimization experiments of the purification were carried out and utilizing these parameters at this step was shown to ensure that the optimal amount of AcrB is extracted from the membrane and proper formation of the native cell membrane nanoparticles occurs. The final critical step of the purification process is loading the sample onto the Ni-NTA column at room temperature. This is necessary, because membrane active polymers are more soluble at room temperature than at 4 °C, thus loading at room temperature will increase the amount of protein binding onto the affinity column and avoid high pressure caused by insoluble polymer buildup that could potentially damage the column. Almost equally as important for obtaining accurate structural information are the steps contained in the negative staining procedure mentioned above. The most critical aspects of this procedure include the use of 10 nm thick holey carbon grids, volumes of water and uranyl acetate, and the lengths of time for sample adsorption and staining. Utilization of these key parameters during sample preparation will ensure quality structural data that can be used for accurate assessment of the oligomeric states of the sample being imaged. Modifications to the purification protocol may be necessary when using different proteins to troubleshoot the problems that may arise due to the unique characteristics of various polypeptides. The primary factors to consider modifying when having difficulty with getting an adequate amount of protein sample should be the parameters

used during the induction step, the amount of membrane fraction used in the solubilization step, and the length of time and temperature for the solubilization process. If there is an issue with purity it may be necessary to utilize alternative affinity columns, such as a biotin affinity column, instead of using the Ni-NTA column for purification. Similarly, if maintenance of weak/transient protein-protein interactions is necessary, exchanging the Ni-NTA column for a TAP-tag affinity column is beneficial for optimum results. Finally, when studying mammalian proteins, mammalian expression systems should be used to maintain true native cell membrane lipid compositions necessary for accurate determination of the natural oligomeric state of the protein. This will require completely revising the protein expression and cell lysis steps of this protocol. In such cases, previously established protocols for protein expression and cell lysis that correspond to the expression system necessary for the target protein of interest should be followed.

Use of the NCMNs with electron microscopy displays great advantages when compared to FRET for use in the detection of PPIs. As the results from this study show, the previously carried out FRET experiments were inconsistent with the structural analysis of the oligomeric structure of the AcrB mutant protein[21]. This was clearly shown and directly confirmed by the images taken with negative stain electron microscopy, which are consistent with the previously described loss of activity for the mutant AcrB-P223G[16]. If AcrB-P223G did form trimers in vivo the NCMNP5-2 polymer would have caught them in the large native cell membrane patches it extracts. It is possible that the FRET analysis of mutant AcrB resulted in a false positive due to any of the several limitations that are intrinsic to the physical processes the technique relies on and the technology utilized to measure the fluorescent resonance energy transfers. One major limitation of FRET is the resolution limits of confocal microscopy and this leads to serious limitations in the intermolecular distances capable of being resolved with FRET assays[19]. In comparison, utilizing NCMNs in conjunction with electron microscopy is not subject to the aforementioned limitation of FRET, with significantly higher resolution limits when compared with those of confocal microscopy. Based on these limitations having potential effects on the previously described FRET assays, we posit that the incorrect detection of an AcrB-P223G trimer in vivo resulted from the low resolution limitation of FRET[21]. Aside from the advantages over just FRET pointed out directly by this paper, using NCMNs in conjunction with electron microscopy has the advantage over all current protein-protein interaction techniques, such as the Y2H system and TAP-MS, in that it can be used to observe protein-protein interactions in native cell membrane environments directly in high resolution and has the potential to be used to determine the protein structures at the atomic level.

Membrane active polymers and electron microscopy are not without limitations as well. Currently, the main issue of NCMN purification is its lower extraction efficiency when compared with detergent-based methods (the polymers in the NCMN library display ~70% the extraction efficiency of DDM). It also has compatibility issues with some affinity columns, such as maltose binding columns. Furthermore, the NCMN purification is still not very successful with highly dynamic membrane proteins or complexes (data unpublished). Utilizing membrane active polymers and electron microscopy for oligomeric state determination experiments requires removal of the proteins from the native cell environment, whereas FRET is carried out in vivo. However, the nanoparticles formed by membrane active polymers allow for the most native-like

environment possible when extracting the proteins from cells, to reduce the potential experimentally derived inaccuracies known to be caused by protein extraction and purification. Additionally, while the issue of resolution and particle size as a limitation of transmission electron microscopy has significantly diminished over the past decade, the microscopes that are still being used for negative stain analysis will still be relatively limited to larger molecules or molecular complexes (>200 kDa) as they generally have an information limit of around 0.1-0.3 nm[25]. SMALP has also shown to be highly flexible in terms of applications but displays even greater limitations than NCMNs. The nanodiscs formed by SMA have a maximum diameter of roughly 15 nm and thus are commonly ineffective for extracting proteins and protein complexes that are over 400 kDa[26]. In addition to this limitation, SMA is also unable to work with proteins that exist in low pH environments or utilize divalent ions for structural and functional purposes. Due to SMALPs mechanism of action being pH dependent, it cannot be used with low pH conditions and chelates divalent ions. While the SMILP and DIBMA methods have offered promise in regards to overcoming these limitations, their applicability to diverse sets proteins has remained unseen[27,28]. NCMNs seeks to overcome these limitations by using structure-activity relationship (SAR) analysis to create alternative polymers that can form larger nanoparticles, functioning in low pH conditions, and avoid chelating divalent ions. One such example of the polymers that have been developed for NCMNs is the NCMNP5-2 polymer which displays the ability to create larger nanoparticles as demonstrated in **Figure 1E,F**.

In addition to the previously described advances in nanoparticle technology, the future direction of NCMNs is in developing even more membrane active polymers that will give the NCMNs polymer library increased extraction efficiency and the ability to work with proteins of all different transmembrane region sizes, that function at much wider pH levels, or rely on any type of ion for maintenance of their structure and function. This will allow for all membrane protein researchers to utilize this technology in their experiments and have access to more accurate and biologically relevant results. By bringing the advantages of polymer nanoparticles to a wider variety of proteins the hope is that this will lead to solving high-resolution structures of native membrane protein complexes at the atomic level and thus determine the intramolecular atomic interactions that go into maintaining these complexes. Such advances would also enable many new possibilities in terms of membrane protein drug discovery and development through structure-based drug design efforts. Utilization of structure-based drug design techniques for membrane proteins would be a massive benefit for the medical industry as this would increase drug binding specificity and efficacy in order to reduce unwanted side effects and the amount of compound necessary to elicit desired therapeutic effects, thus making drugs that target membrane proteins significantly safer and more effective. The native cell membrane nanoparticles system is still in its developmental stages but has already proven to be incredibly powerful by allowing for the first time the study of membrane proteins in their truly native states and elucidating the native protein-protein interactions that occur on the cell membrane.

ACKNOWLEDGMENTS:

This research was supported by VCU startup fund (to Y.G.) and National Institutes of Health via Grant R01 1GM132329-01 (to Y.G.)

DISCLOSURES:

Y.G is listed as inventor of the membrane active polymer NCMNP5-2 and NCMN system.

REFERENCES:

1. Berggard, T., Linse, S., James, P. Methods for the detection and analysis of protein-protein interactions. *Proteomics.* **7** (16), 2833-2842 (2007).
2. Huang, H., Bader, J. S. Precision and recall estimates for two-hybrid screens. *Bioinformatics.* **25** (3), 372-378 (2009).
3. Serebriiskii, I. G., Golemis, E. A. Two-hybrid system and false positives. Approaches to detection and elimination. *Methods in Molecular Biology.* **177**, 123-134 (2001).
4. Gingras, A. C., Gstaiger, M., Raught, B., Aebersold, R. Analysis of protein complexes using mass spectrometry. *Nature Reviews in Molecular Cell Biology.* **8** (8), 645-654 (2007).
5. Ngounou Wetie, A. G. et al. Investigation of stable and transient protein-protein interactions: Past, present, and future. *Proteomics.* **13** (3-4), 538-557 (2013).
6. Schaufele, F. Maximizing the quantitative accuracy and reproducibility of Forster resonance energy transfer measurement for screening by high throughput widefield microscopy. *Methods.* **66** (2), 188-199 (2014).
7. Berney, C., Danuser, G. FRET or no FRET: a quantitative comparison. *Biophysical Journal.* **84** (6), 3992-4010 (2003).
8. Almen, M. S., Nordstrom, K. J., Fredriksson, R., Schioth, H. B. Mapping the human membrane proteome: a majority of the human membrane proteins can be classified according to function and evolutionary origin. *BMC Biology.* **7**, 50 (2009).
9. Overington, J. P., Al-Lazikani, B., Hopkins, A. L. How many drug targets are there? *Nature Reviews in Drug Discovery.* **5** (12), 993-996 (2006).
10. Berman, H. M. et al. The Protein Data Bank. *Nucleic Acids Research.* **28** (1), 235-242 (2000).
11. Overduin, M., Esmaili, M. Memtein: The fundamental unit of membrane-protein structure and function. *Chemistry and Physics of Lipids.* **218**, 73-84 (2019).
12. Qiu, W. et al. Structure and activity of lipid bilayer within a membrane-protein transporter. *Proceedings of the National Academy of Sciences U. S. A.* **115** (51), 12985-12990 (2018).
13. Knowles, T. J. et al. Membrane proteins solubilized intact in lipid containing nanoparticles bounded by styrene maleic acid copolymer. *Journal of the American Chemical Society.* **131** (22), 7484-7485 (2009).
14. Xue, M., Cheng, L., Faustino, I., Guo, W., Marrink, S. J. Molecular Mechanism of Lipid Nanodisk Formation by Styrene-Maleic Acid Copolymers. *Biophysical Journal.* **115** (3), 494-502 (2018).
15. Parmar, M. et al. Using a SMALP platform to determine a sub-nm single particle cryo-EM membrane protein structure. *Biochimica and Biophysica Acta Biomembrames.* **1860** (2), 378-383 (2018).
16. Yu, L., Lu, W., Wei, Y. AcrB trimer stability and efflux activity, insight from mutagenesis studies. *PLoS One.* **6** (12), e28390 (2011).
17. Broussard, J. A., Rappaz, B., Webb, D. J., Brown, C. M. Fluorescence resonance energy

transfer microscopy as demonstrated by measuring the activation of the serine/threonine kinase Akt. *Nature Protocols.* **8** (2), 265-281 (2013).
18. Ma, L., Yang, F., Zheng, J. Application of fluorescence resonance energy transfer in protein studies. *Journal of Molecular Structure.* **1077**, 87-100 (2014).
19. Sachl, R., Humpolickova, J., Stefl, M., Johansson, L. B., Hof, M. Limitations of electronic energy transfer in the determination of lipid nanodomain sizes. *Biophysical Journal.* **101** (11), L60-62 (2011).
20. Woehler, A., Wlodarczyk, J., Neher, E. Signal/noise analysis of FRET-based sensors. *Biophysical Journal.* **99** (7), 2344-2354 (2010).
21. Wang, Z. et al. Comparison of in vitro and in vivo oligomeric states of a wild type and mutant trimeric inner membrane multidrug transporter. *Biochemical and Biophysical Reports.* **16** 122-129 (2018).
22. Scarff, C. A., Fuller, M. J. G., Thompson, R. F., Iadaza, M. G. Variations on Negative Stain Electron Microscopy Methods: Tools for Tackling Challenging Systems. *Journal of Visualized Experiments.* (132), e57199 (2018).
23. Lu, W., Zhong, M., Wei, Y. Folding of AcrB Subunit Precedes Trimerization. *Journal of Molecular Biology.* **411** (1), 264-274 (2011).
24. Lebon, G. *Structure and Function of GPCRs*. 229-230 (Springer International Publishing, 2019).
25. Rames, M., Yu, Y., Ren, G. Optimized negative staining: a high-throughput protocol for examining small and asymmetric protein structure by electron microscopy. *Journal of Visualized Experiments.* (90), e51087 (2014).
26. Lee, S. C. et al. A method for detergent-free isolation of membrane proteins in their local lipid environment. *Nature Protocols.* **11** (7), 1149-1162 (2016).
27. Hall, S. C. L. et al. An acid-compatible co-polymer for the solubilization of membranes and proteins into lipid bilayer-containing nanoparticles. *Nanoscale.* **10** (22), 10609-10619 (2018).
28. Oluwole, A. O. et al. Solubilization of Membrane Proteins into Functional Lipid-Bilayer Nanodiscs Using a Diisobutylene/Maleic Acid Copolymer. *Angewandte Chemie International Edition England.* **56** (7), 1919-1924 (2017).

Figure 1

Click here to access/download;Figure;Figure 1.tif

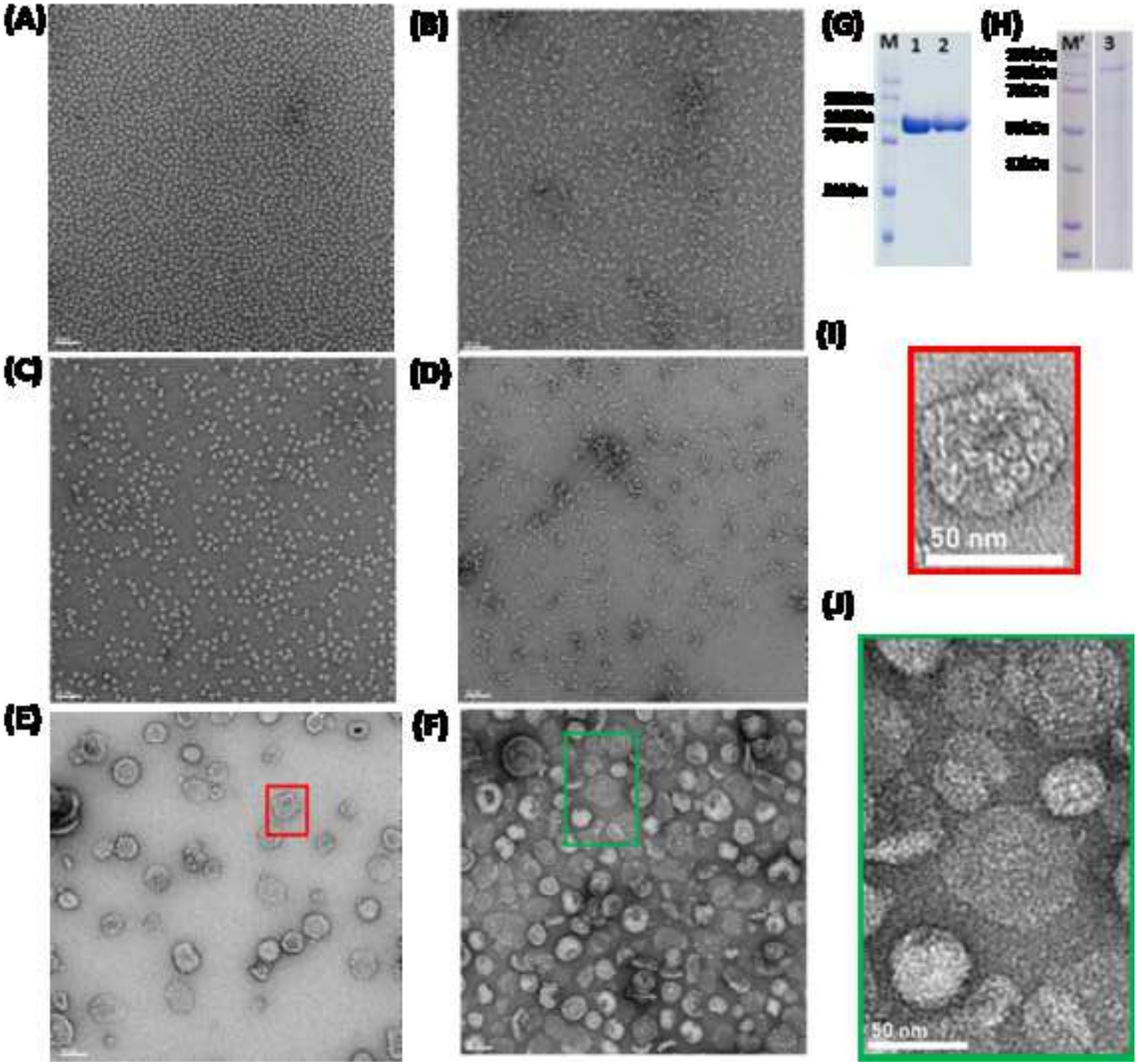

Table of buffers

Click here to access/download;Table of Materials;Jove_Purification_Buffer_Table.xlsx

DDM Purification Buffers		Polymer Purification Buffers	
Buffer A	50 mM HEPES, pH 7.8 300 mM NaCl 5% Glycerol 20 mM Imidazole 1 mM $MgCl_2$-6 H_2O 0.1 mM TCEP	**NCMN Buffer A**	50 mM HEPES, pH 8.4 500 mM NaCl 5% Glycerol 20 mM Imidazole 0.1 mM TCEP
Buffer B	50 mM HEPES, pH 7.8 300 mM NaCl 5% Glycerol 40 mM Imidazole 1 mM $MgCl_2$-6 H_2O 0.1 mM TCEP	**NCMN Buffer B**	25 mM HEPES, pH 7.8 500 mM NaCl 5% Glycerol 40 mM Imidazole 0.1 mM TCEP
Buffer C	50 mM HEPES, pH 7.8 300 mM NaCl 5% Glycerol 75 mM Imidazole 1 mM $MgCl_2$-6 H_2O 0.1 mM TCEP	**NCMN Buffer C**	25 mM HEPES, pH 7.8 500 mM NaCl 5% Glycerol 75 mM Imidazole 0.1 mM TCEP
Buffer D	50 mM HEPES, pH 7.8 300 mM NaCl 5% Glycerol 300 mM Imidazole 1 mM $MgCl_2$-6 H_2O 0.1 mM TCEP	**NCMN Buffer D**	25 mM HEPES, pH 7.8 500 mM NaCl 5% Glycerol 300 mM Imidazole 0.1 mM TCEP
Buffer E	40 mM HEPES, pH 7.8 200 mM NaCl 0.1 mM TCEP	**NCMN Buffer E**	40 mM HEPES, pH 7.8 200 mM NaCl 0.1 mM TCEP

Gel Electrophoresis Buffers	
TAE Buffer	40 mM Tris Base 1 mM EDTA 20 mM Acetic Acid
Destaining Buffer	40% Methanol 10% Acetic Acid
Stacking Gel	1.5 M Tris pH 8.8 (0.63 ml) 30% Acrylamide/Bis (0.43 ml) 10% SDS (0.025 ml) 10% APS (0.025 ml) TEMED (4 µl) H_2O (1.39 ml)
12% Separating Gel	1.5 M Tris pH 8.8 (1.3 ml) 30% Acrylamide/Bis (2 ml) 10% SDS (0.05 ml) 10% APS (0.05 ml) TEMED (5 µl) H_2O (1.6 ml)

Name of Material/Equipment
Chemicals
30% Acrylamide/BIS SOL (37.5:1)
4x Laemmli Sample Buffer (Loading Buffer)
Acetic Acid Glacial
Ammonium Persulfate (APS)
Chloramphenicol
Coomassie Brilliant Blue R-250 protein stain powder
DTT (Dithiothreitol) (> 99% pure) Protease free
Glycerol
HEPES
Imidazole
IPTG
Kanamycin
Magnesium chloride hexahydrate
Methanol
N,N-dimethylethylenediamine (EDTA)
NCMNS-P5-2
Precision Plus Protein Dual Color Standard
SDS (Sodium Dodecyl Sulfate)
SMA2000
Sodium Chloride
TCEP-HCl
TEMED
Terrific Broth Media
Tris Base
Uranyl Acetate
Equipment
Avanti J-26S XPI
Avanti JXN-30
Carbon Electron Microscope Grids (10 nm)
Con-Torque Tissue Homogenizer

Corning LSE Mini Microcentrifuge
EmulsiFlex-C3
Fraction Collector F9-R
Mini-PROTEAN Tetra Vertical Electrophoresis Cell
NanoDrop 2000 Spectrophotometer
Optima L-90K Ultracentrifuge
PELCO easiGlow Glow Discharge Cleaning System
Potter-Elvehjem Safe Grind Tissue Grinder
PowerPac Basic Power Supply
Razel R99-E Variable Speed Syringe Pump
Superdex 200 Increase 10/300 GL
Tecnai F20 200kV
Type 70 Ti Fixed-Angle Rotor
General Materials
1.5 ml Microcentrifuge Tubes
4 ml Amicon Ultra-4 30 kDa
AKTA pure 25 L1 FPLC
BL21(DE3)pLysS Cells
Falcon 50 ml Conical Centrifuge Tube
HisTrap HP 5 ml Column
pET-24a

Company	Catalog Number
Bio-Rad	161-0158
Bio-Rad	1610747
ThermoFisher Scientific	A38S-212
Bio-Rad	161-0700
Goldbio	C-105-5
Bio-Rad	161-0400
Goldbio	DTT10
ThermoFisher Scientific	G33-4
ThermoFisher Scientific	BP310-1
Affymetrix	17525 1 KG
Goldbio	I2481C100
Goldbio	K-120-25
ThermoFisher Scientific	AA3622636
ThermoFisher Scientific	A412-4
Merck	8.03779.0100
Not commercially available yet	Submit request for obtaining to corresponding author
Bio-Rad	161-0374
Bio-Rad	161-0301
Cray Valley	Submit request for obtaining to corresponding author
ThermoFisher Scientific	S271-10
Goldbio	TCEP25
Bio-Rad	161-0800
Affymetrix	75856 1 KG
Bio-Rad	161-0719
Ambinter	Amb22348393
Beckman Coulter	B14538
Beckman Coulter	B34193
Electron Microscopy Sciences	CF300-Cu-TH
Eberbach	E7265

ThermoFisher Scientific	07-203-954
Avestin	
GE Healthcare Life Sciences	29003875
Bio-Rad	165-8004
ThermoFisher Scientific	ND-2000
Beckman Coulter	PN LL-IM-12AB
Ted Pella	91000S-230
Wheaton	358013
Bio-Rad	164-5050
Razel Scientific Instruments	
GE Healthcare Life Sciences	28990944
FEI	
Beckman Coulter	
ThermoFisher Scientific	05-408-129
Millipore Sigma	UFC803024
GE Healthcare Life Sciences	29018225
ThermoFisher Scientific	C606003
ThermoFisher Scientific	14-959-49A
GE Healthcare Life Sciences	17524802
EMD Biosciences	69749-3

Comments/Description

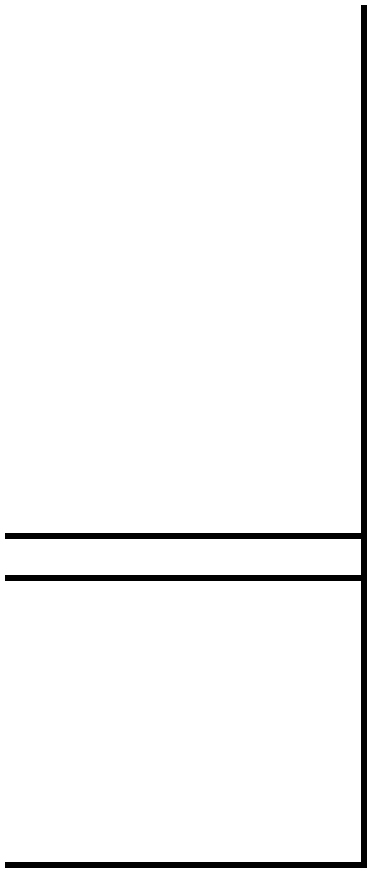

Editorial comments:

1. The editor has formatted the manuscript to match the journal style. Please retain and use the attached file for revision.

The journal style is retained.

2. Please address all the specific comments marked in the manuscript.

All comments have been addressed.

3. Some of the claims are still not supported with data. Also not presenting the details about the polymer doesn't bring out clarity. Please further reduce the scope of the manuscript or include additional details to support the claims.

This has been addressed in the revised manuscript and responses to the comments.

Detailed polymer information is beyond the scope of this manscript. Here we just show how to use these polymers.

4. The manuscript needs thorough proofreading.

It has been done.

5. Once done please highlight 2.75 pages of the protocol which forms a cohesive story and is in line with the title of the protocol for filming purpose.

This has been done.

Reviewer #1:
Manuscript Summary:
This is sufficient

Major Concerns:
NA

Minor Concerns:
There are still some minor concerns that without the accompanying manuscript on the polymers some of the data is not supported as well as it could be. This would be a good partner manuscript to that paper and provide a more practical paper on how to work with the polymer.

I agree. Ideally, we should published our result oriented manuscript first.

Reviewer #2:
Thanks for your responses to the concerns I raised. My mind is very much set at rest by seeing the SEC profiles of the samples used for EM. It is critical to include these in your data and the description of the results.

We included the SEC data in the manuscript.

Major Concerns:
Specific comments
1. Authors said: From line 195 to line 244, Protocol section 3. Preparation of Native Cell Membrane Nanoparticles details the SMALP purification. In our NCMN system, both SMA2000 and NCMNP5-2 are membrane active polymers. The resulting samples in our NCMN system are called Native Cell Membrane Nanoparticles.

- It seems that we are at odds over terminology. In order to make the protocol completely clear to the reader, please call section 3. Preparation of Native Cell Membrane Nanoparticles and SMALPs. I understand that you consider NCMNs and SMALPs to be part of the same family but like me, other readers may not yet have made this connection.

Our NCMN system was inspired by the SMALP system, but they are quite different. We detailed in the revised manuscript in the part of introduction.

2. Authors said: the reasons why we didn't show the SEC profile of WT AcrB and AcrB-P223G with DDM purification is that this has been reported in the article where the FRET analysis of AcrB-P223G was done. Their SEC analysis of AcrB-P223G suggests majority of AcrB-P223G exists as monomer. Our SEC profile below agrees with their report.

- As I stated above, this figure needs to be included in your data, along with an indication of the column calibration. I understand that this is not novel data, as it has been previously reported, but it shows that you have replicated the previous study and is a measure of quality control for the samples that you image by EM.

We included it in the revised manuscript.

3. Authors said: The apparent difference in protein concentration is hard to control. The concentration (in our experimental conditions) of WT AcrB or AcrB-P223G is not significant factor that affect the oligomeric states. Our SEC profile as provided above also support my argument that majority of WT AcrB molecules exist as a trimer, and

majority of AcrB-P223G molecules exist as monomer weather in DDM, SMA or cell membrane environment.

- I agree with your points about the concentration-dependence of oligomerisation. My concern was about the appearance of the micrographs and how easy they are for the reader to interpret. Diluting the samples to achieve better particle spacing would have been useful, but I understand that it may be a difficult undertaking at this point. The addition of the SEC data satisfies me on this point because it shows a clear difference between the samples that supports the interpretation of the EM images.

Great. I hope the included SEC data will be helpful for other readers too.

4. Authors said: I agree with you that this is negative stain images at low resolution. However, because AcrB trimers are large enough to be observable at this magnification (62000X) with CCD detector in the negative stain condition (as you also agreed you were able to see some AcrB-like particles in the WT samples). In Figure 1I, both you and us could not see similar AcrB trimer particles. This images is just a representative images we had taken. We didn't show all of them, but we did check other images of the AcrB-P223G samples, we could not find observable AcrB trimer as that from WT AcrB samples. Because these large lipid bilayer patches are purified with His-affinity column, the majority of these patches should contain AcrB-P223G molecules. We see His-tagged wild type AcrB trimer particles in the large lipid bilayer patches but did not observe His-Tagged AcrB-P223G in the large lipid bilayer patches. The conclusion will naturally be that AcrB-P223G molecules do not exist as trimers. I also want to point out that, it is possible that some of the large lipid bilayer patches may do contain some WT AcrB trimers or AcrB-P223G trimers, but the amount is extremely small. The large patch may randomly catch some WT AcrB trimer particles together with AcrB-P223G. There may even be a very small amount of AcrB-P223G molecules that do exists as trimer, but considering the comparative results, our data still strongly suggest Acrb-P223G exists on the cell membrane as monomer rather than trimer. We have to admit that we could not rule out that very small amount of AcrB-P223G may exist as trimer in the cell membrane. That is beyond of the capability of our approaches and sticking to that possibility will not help answering the real question we are trying to answer: does the membrane environment favor the trimerization of AcrB-P223G? Our conclusion is No, the cell membrane environment does not help the trimerization of AcrB-P223G. In principle, P223G mutation leads to conformational change of the loop region that is crucial for trimerization. It is the structural differences that dictates that wild type AcrB monomers come together to form trimers, and AcrB-P223G monomers preferentially exist as monomers, comparing with the lipid environmental factor, the intrinsic structural difference is more important.

- I have not been very here precise in my use of language to describe my concerns, and I apologise for that. I was not criticising the use of neg stain EM as a method. I meant that the pictures shown in the figure are somewhat pixelated. On their own I do not find them compelling. Once again, this concern has been addressed by the addition of the SEC data.

Ok. We are glad to know that the combination of the EM image and SEC data is more helpful.

Reviewer #3:
Manuscript Summary:
This revision is appropriate for publication, and will be of significant interest to membrane biologists.

Thank you.

Major Concerns:
none

Minor Concerns:
none

(A)

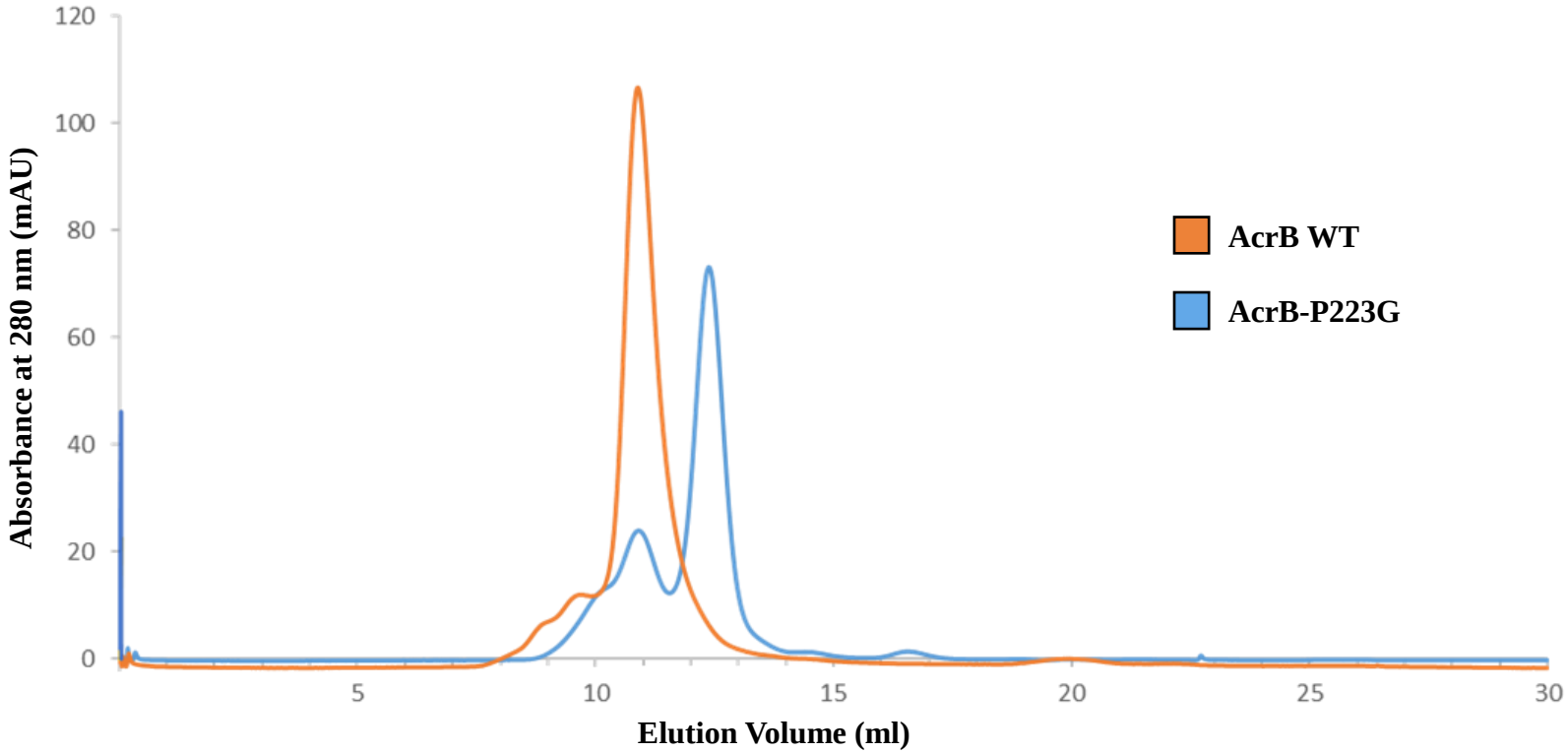

(B)